ORIGINAL PAPER

Improved properties of polymer electrolyte by ionic liquid PP1.3TFSI for secondary lithium ion battery

An Yongxin · Cheng Xinqun · Zuo Pengjian · Liao Lixia · Yin Geping

Abstract A new kind of polymer electrolyte is prepared from *N*-methyl-*N*-propylpiperidinium bis (trifluoromethanesulfonyl) imide (PP1.3TFSI), polyethylene oxide (PEO), and lithium bis (trifluoromethanesulfonyl) imide (LiTFSI). IR and X-ray diffraction results demonstrate that the addition of ionic liquid decreases the crystallization of PEO. Thermal and electrochemical properties have been tested for the solid polymer electrolytes, the addition of the room temperature molten salt PP1.3TFSI to the conventional $P(EO)_{20}LiTFSI$ polymer electrolyte leads to the improvement of the thermal stability and the ionic conductivity ($x=1.27$, 2.06×10^{-4} S cm^{-1} at room temperature), and the reasonable lithium transference number is also obtained. The Li/LiFePO$_4$ cell using this polymer electrolyte shows promising reversible capacity, 120 mAh g^{-1} at room temperature and 164 mAh g^{-1} at 55 °C.

Keywords Li-ion battery · Ionic liquids · Conductivity · Polymer electrolytes

Introduction

Solid-state polymer electrolytes (SPEs) are widely investigated in the lithium ion battery because they have many unique properties such as plasticity and thermal stability. Especially, they attract more attention when applied in the power source of electric vehicle and hybrid electric vehicle. However, the low ionic conductivity of SPEs (~1×10^{-5} S cm^{-1} or even lower) at room temperature, which is about three decades lower than that of the conventional liquid electrolyte, restricts their application in lithium ion battery [1–3]. Several approaches have been developed to improve their room temperature ionic conductivity: (1) employing lithium salts with large and flexible anions (e.g., lithium bis (trifluoromethanesulfonyl) imide, LiTFSI) [4]; (2) mixing high conductivity inorganic nano-fillers [5]; (3) incorporating liquid organic solvents (EC, PC) [6]; (4) adopting amorphous, low molecular-weight polymers (e.g., PEGDME) [7]. The former two approaches can enhance the conductivity of polymer electrolytes a bit at room temperature, but the values are still far for practical applications. On the other hand, the latter two approaches also sacrifice the safety due to the flammability of liquid organic solvents.

Room temperature ionic liquids (RTILs) have been investigated for decades as electrolyte components in electrochemical devices due to their well-known advantages: high ionic conductivity, non-flammability, wide electrochemical stability window, and environmentally benign nature [8–11]. Midazolium cation, 1-ethyl-3-methyl imidazolium bis (trifluoromethanesulfonyl) imide has been intensively studied by virtue of low viscosity [12, 13]. However, the stability of this kind of IL against the reduction potential (about 1 V vs. Li/Li$^+$) cannot meet the need of the lithium ion battery. Matsumoto et al. [14] found that quaternary ammonium-imide salts have high cathodic stability against lithium metal. For example, PYR14TFSI can improve the electrochemical stability and the ionic conductivity of the polymer electrolytes remarkably at room temperature [15].

Compared with PYR14TFSI, *N*-methyl-*N*-propylpiperidinium bis (trifluoromethanesulfonyl) imide (PP1.3TFSI) has the stability reduction potential (about −0.3 V vs. Li/Li$^+$) and higher conductivity (about 2.3 mS cm^{-1}, while the

A. Yongxin · C. Xinqun · Z. Pengjian · L. Lixia · Y. Geping (✉)
School of Chemical Engineering and Technology,
Harbin Institute of Technology,
No. 92, West Da-Zhi Street,
Harbin 150001, China
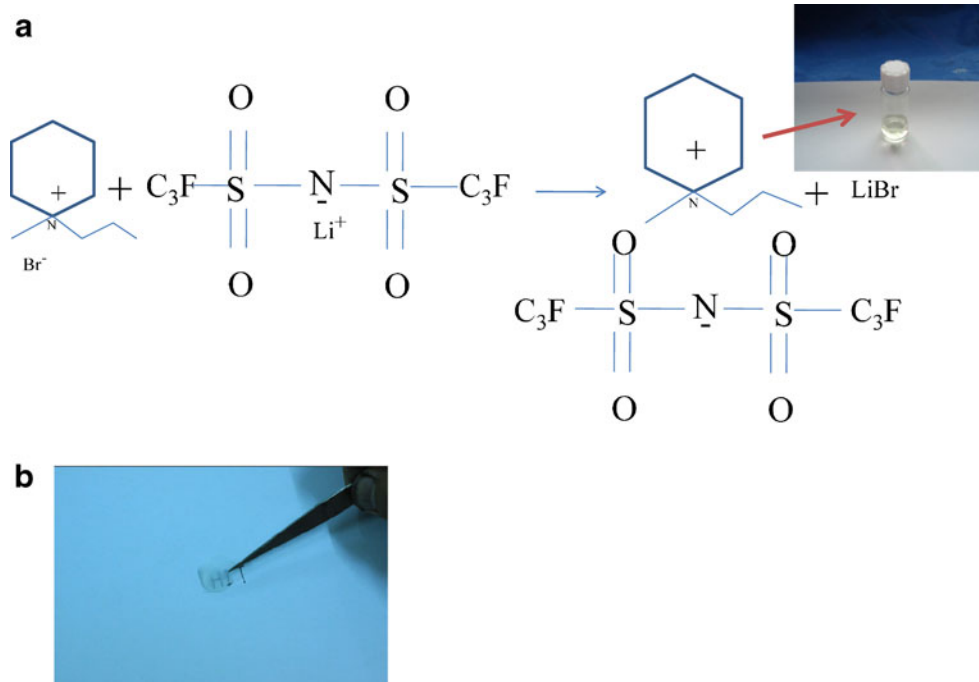e-mail: yingeping2006@163.com

PYR14TFSI is only 1.3 mS cm^{-1}) [16]. In this paper, we succeeded to synthesize PP1.3TFSI and demonstrate the feasibility of PP1.3TFSI in enhancing the ionic conductivity of polyethylene oxide (PEO)-based electrolytes at room temperature without suppressing the electrochemical stability of the polymer electrolyte. The PP1.3TFSI-LiTFSI-PEO polymer electrolyte system was characterized in terms of ionic conductivity and thermal stability. Preliminary performance was also tested by Li/PP1.3TFSI-LiTFSI-P(EO)$_{20}$/LiFePO$_4$ cell at room temperature and 55 °C.

Experimental

Preparation of polymer electrolytes

PEO, Mw=3×10^6 (Aldrich), LiTFSI (99%, TCI), and PP1.3Br (99%, Meisibei Shanghai) were dried under vacuum for 48 h (PEO and PP1.3Br at 50 °C, LiTFSI at 150 °C). Dissolving LiTFSI and PP1.3Br (1:1 mole ratio) separately in deionized H$_2$O and combining gave the pure PP1.3TFSI, which was phase-separated from the aqueous layer (LiBr dissolved in the aqueous layer). The PP1.3TFSI was collected and washed several times with deionized H$_2$O. The final aqueous layer was removed and the PP1.3TFSI was purified by activated carbon (Cabot), and then dried under vacuum at 100 °C for 24 h and then 130 °C for 6 h. The resulting PP1.3TFSI salt is a clear, colorless liquid at room temperature and was stored/handled in a glove box. The IL here developed (PP1.3TFSI) was synthesized according to the route Scheme 1a.

Solvent-free P(EO)$_{20}$LiTFSI+xPP1.3TFSI (x is mole rate of PP1.3$^+$/Li$^+$, x=0, 0.54, 0.96, 1.27) electrolytes were prepared as follows: PEO and LiTFSI (EO/Li$^+$=20) were first mixed in a mortar and then PP1.3TFSI was added to the mixture to achieve the selected mole ratio. Then the polymer electrolytes were annealed under vacuum at 90 °C overnight. A thin film (100 μm) was obtained by hot pressing of the polymer electrolytes at 115 °C for 2 min (Scheme 1b).

Measurements

The decomposition temperature of P(EO)$_{20}$LiTFSI+xPP1.3TFSI electrolytes was investigated by thermal gravimetry (TG, PerkinElmer Diamond), recording the weight loss from 25 up to 500 °C at 5 °C min^{-1}. The flaming ability of electrolyte was testified by burning tests. A lighter was used to burn one end of electrolyte film (Φ=1.44 cm), and the light was removed from under the electrolyte film after 5 s. The electrolyte was judged to be nonflammable if the electrolyte never ignited during the testing or if the ignition of electrolyte ceased when the flame was removed. Each electrolyte was tested three times. FT-IR analysis of polymer electrolytes was carried out by using the PerkinElmer Spectrum100 in the wave region of 4,000~400 cm^{-1} at room temperature at 4 cm^{-1} resolution.

X-ray diffraction (XRD) patterns were acquired by using a Rigaku diffractometer with Cu Kα radiation at a scanning rate of 2°/min. The microscopic morphologies of the polymer electrolytes were obtained using scanning electron

Scheme 1 Preparation of the a PP1.3TFSI and b photo of P(EO)$_{20}$LiTFSI-PP1.3TFSI electrolyte film

microscopy (SEM, HITACHI S4700). Linear sweep voltammograms for polymer electrolytes were measured on Pt/polymer electrolyte/Li cell by electrochemical analyzer (CHI604B). The ionic conductivity of polymer electrolyte was measured by impedance spectroscopy, performed on a two stainless steel disks electrodes.
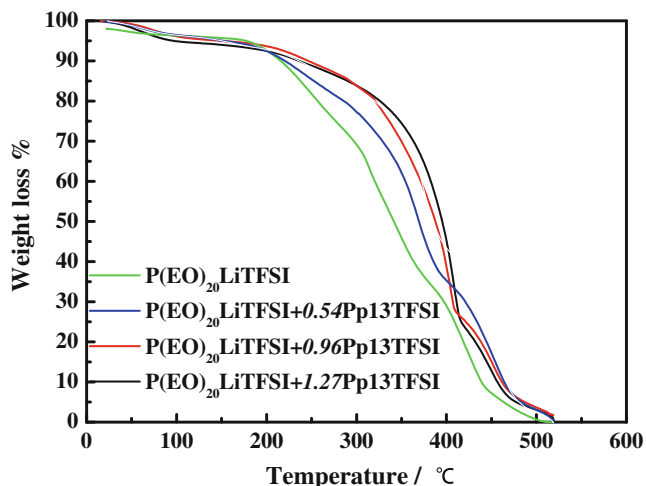
The lithium transference number was determined by a dc polarization combined with impedance spectroscopy following the technique proposed by Bruce et al. [17, 18]; dc polarization and impedance spectroscopy were tested by CHI604B. The Li/P(EO)$_{20}$LiTFSI+PP1.3TFSI/LiFePO$_4$ cell was assembled in a glove box by contacting a lithium foil anode, a P(EO)$_{20}$LiTFSI+1.27PP1.3TFSI film electrolyte and a lithium iron phosphate cathode in sequence. The voltage region of the cell was 2.0~4.0 V (vs. Li/Li$^+$).
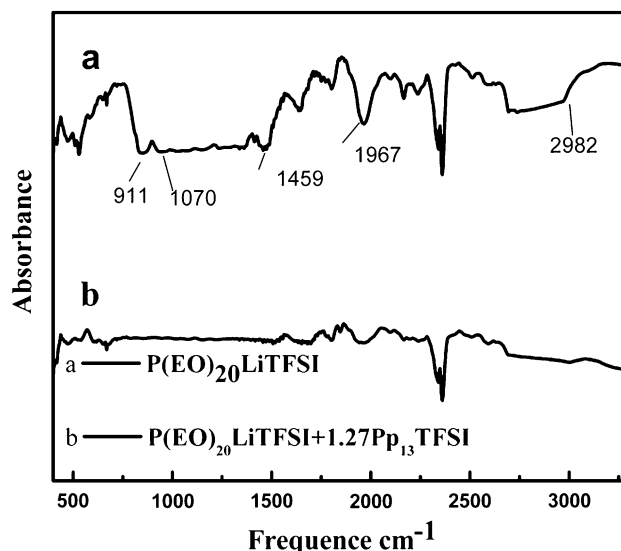
Results and discussion

Thermal gravimetric analysis of the electrolytes at air atmosphere is shown in Fig. 1. It is seen that initial degradation temperature (T_i) of the ionic liquid-free polymer is lower than 200 °C. P(EO)$_{20}$LiTFSI+0.96PP1.3TFSI polymer electrolyte has better thermal stability than P(EO)$_{20}$LiTFSI, whose thermal stability is higher than 220 °C. The initial degradation temperature of polymer contain 1.27PP1.3TFSI is even higher.

The flaming test showed that P(EO)$_{20}$LiTFSI got burning in the first second of ignition and lasted for more than 30 s. In contrast to this behavior, P(EO)$_{20}$LiTFSI+1.27PP13TFSI did not show any combustion even after more than 10 s of flame exposure, indicating that safety can be improved in polymer electrolyte system by PP1.3TFSI.

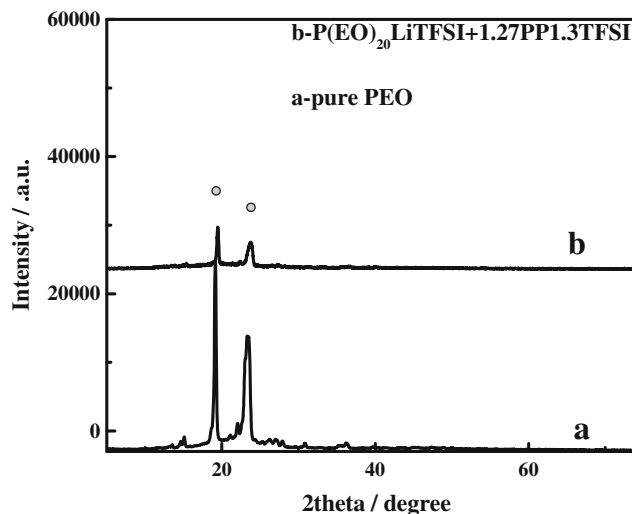The FT-IR spectra of P(EO)$_{20}$LiTFSI+xPP1.3TFSI (x=0, 1.27) are shown in Fig. 2. The band assignments for IL-free PEO-LiTFSI system are taken from previous studies. CH stretching mode can be observed at 2,981 cm^{-1}, asymmetric stretching mode at 1,968 cm^{-1}, CH$_2$ scissoring mode at 1,474 cm^{-1}, C-O-C stretching mode at 1,101 cm^{-1}, CH$_2$ twisting mode at 961 cm^{-1}, and CH$_2$ wagging mode at 841 cm^{-1} [19]. The addition of PP13TFSI in PEO-LiTFSI system results in changes of adsorption peaks (2,981, 1,968, 1,474, 1,101, and 961 cm^{-1} shift to 2,979, 1,961, 1,526, 1,056, and 894 cm^{-1}) and lowering the intensity of adsorption. These changes are caused by the diffusion of IL to PEO-LiTFSI system by reducing the Li-O bond energy and decreasing the crystallization of PEO, which have positive effect on the P(EO)$_{20}$LiTFSI electrolytes.

Figure 3 shows the XRD patterns of PEO, P(EO)$_{20}$LiTFSI+1.27 PP1.3TFSI. Pure PEO shows diffraction peaks at 2θ =19.5°, 23.8°. Meanwhile, the intensity of diffraction

Fig. 2 FT-IR spectra of P(EO)$_{20}$LiTFSI+xPP1.3TFSI (x=0, 1.27)

Fig. 1 Thermal gravimetric analysis (TGA) curves of P(EO)$_{20}$LiTFSI with different mol rate PP1.3TFSI polymer electrolytes

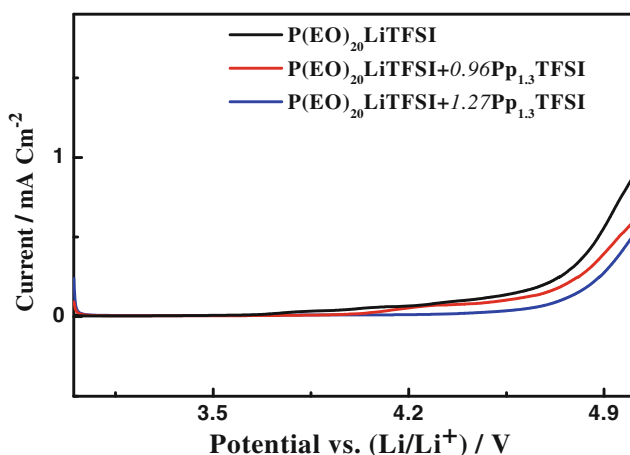**Fig. 3** The XRD patterns of selected polymer electrolytes

Fig. 4 SEM images of the P(EO)$_{20}$LiTFSI with **a** 0 and **b** *1.27*PP1.3TFSI
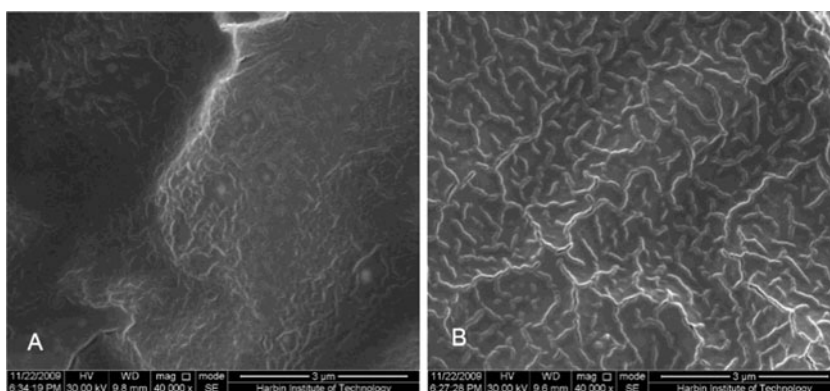
peaks for P(EO)$_{20}$LiTFSI+*1.27*PP1.3TFSI becomes weaker, indicating that the addition of IL lowers the crystallization of PEO. Based on the calculation of MDI Jade 5.0 program, the crystallization degree of P(EO)$_{20}$LiTFSI+*1.27*PP1.3TFSI was estimated to be only 15% of pure PEO.

Figure 4 presents the SEM images of polymer electrolytes with/without PP1.3TFSI. In P(EO)20LiTFSI+*1.27*PP1.3TFSI system, complexes of high-molecular-weight PEO and inorganic alkali metal salts typically have spherulitic morphologies, which have diameter ranging from a few micrometers to several centimeters (Fig. 4b) [20], while ionic liquid-free sample shows irregular and poriferous morphologies (Fig. 4a).

Figure 5 presents the linear sweep voltammograms of P(EO)$_{20}$LiTFSI with different amounts of PP1.3TFSI. Good anodic stability are seen for ionic liquid-polymer electrolytes, ionic liquid-free sample P(EO)$_{20}$LiTFSI the oxidation potential is 4.5 V(vs.Li/Li$^+$), with the increasing mol ratio of PP1.3TFSI, the electrochemical stability of polymer electrolytes also increase a bit. P(EO)$_{20}$LiTFSI+*1.27*PP1.3TFSI

oxidation potential is observed at 4.7 V (vs. Li/Li$^+$), it is a acceptable value for practical application in lithium batteries.

In order to determine the ionic conductivity, ternary polymer electrolyte was sandwiched between two parallel
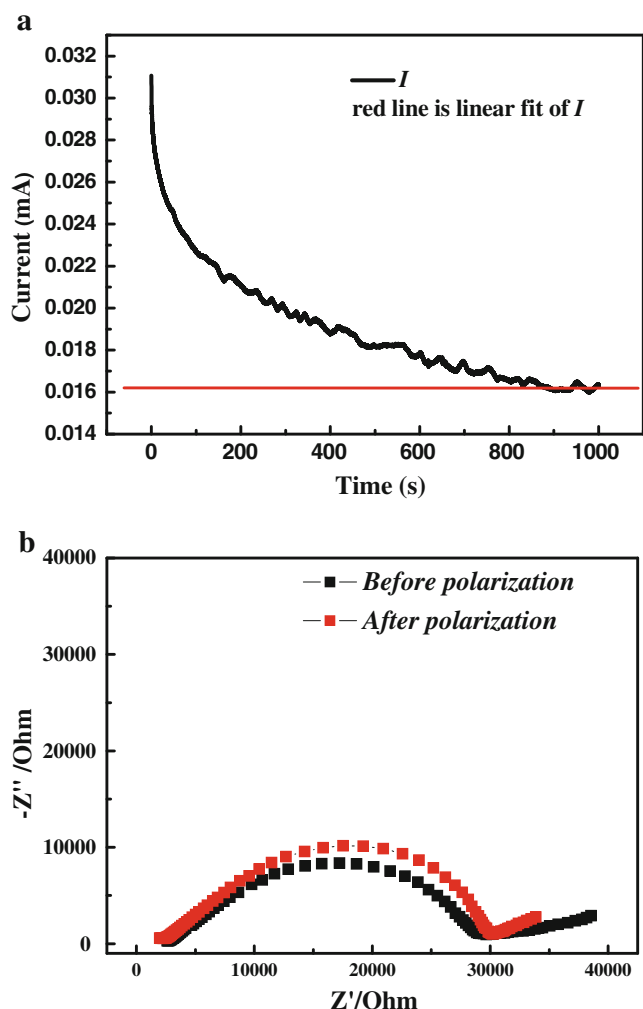

Fig. 5 Linear sweep voltammograms on stainless steel for P(EO)$_{20}$ LiTFSI with 0, 0.96, and 1.27 ionic liquid PP1.3 TFSI as matrixes; scanning rate is 1 mV s^{-1}
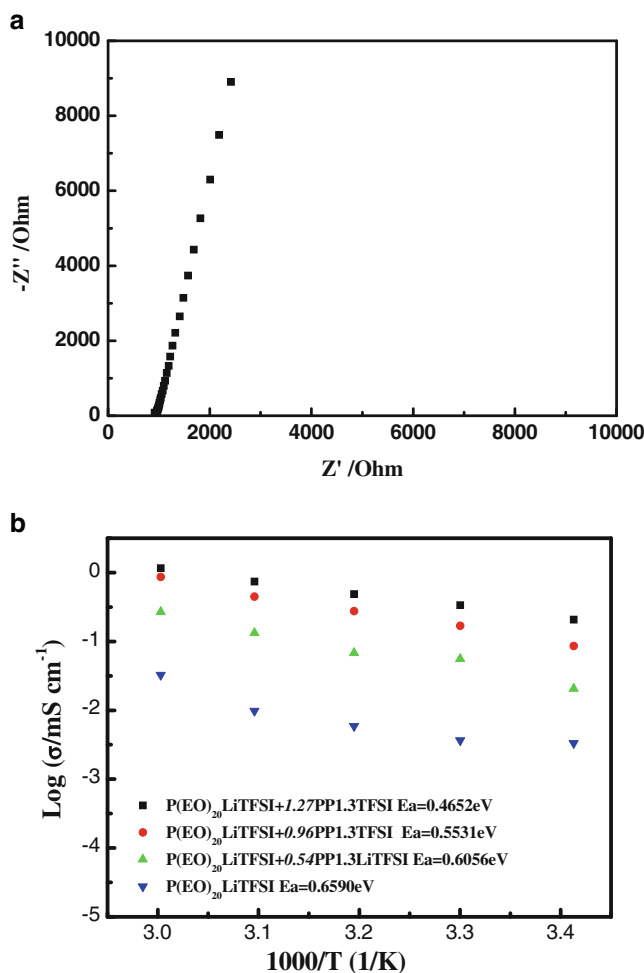
Fig. 6 a The Nyquist plot of the cell SS/P(EO)$_{20}$LiTFSI+ *1.27*PP1.3TFSI/SS at room temperature. **b** Temperature dependence of the ionic conductivity of P(EO)$_{20}$LiTFSI+*x* PP1.3TFSI (*x*=0, 0.54, 0.96, 1.27) polymer electrolytes
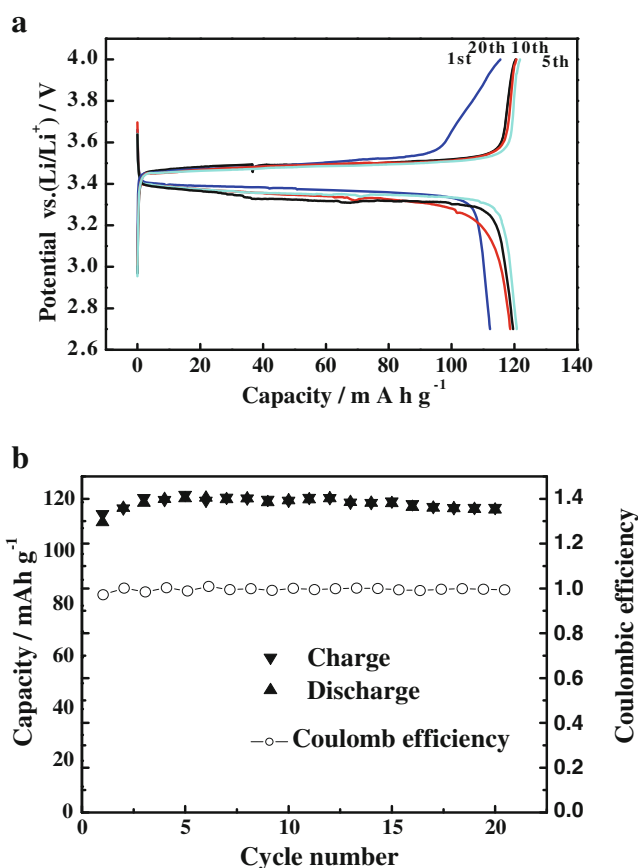
Fig. 8 The voltage–capacity plots and cycle performance of Li/LiFePO$_4$ cell using P(EO)$_{20}$LiTFSI+1.27PP1.3TFSI electrolyte

Fig. 7 a Chronoamperometry of the cell with P(EO)$_{20}$LiTFSI+ PP1.3TFSI at 20 °C ΔV=0.010 Vdc pulse. b Impedance response of the same cell before and after the dc polarization

stainless steel disks (Φ=1 cm). The ionic conductivity was calculated from the following Eq. (1):

$$\delta = \frac{L}{RS} \quad (1)$$

Figure 6a presents the Nyquist plot of P(EO)$_{20}$ LiTFSI+1.27PP1.3TFSI at room temperature. The intersection of the straight line with the real part axis is the bulk electrolyte resistance (R), L is the thickness of polymer electrolyte, and S is the area of stainless steel disks.

The addition of ionic liquid largely increased the conductivity of polymer electrolytes P(EO)$_{20}$LiTFSI and the sample with x=1.27 shows the highest conductivity of ~2.06× 10^{-4} S cm^{-1}, while the conductivity value of P(EO)$_{20}$LiTFSI is only 3.95×10^{-6} S cm^{-1} at room temperature. At 60 °C, conductivity of the sample x=1.27 is 8.68×10^{-4} S cm^{-1}, while the ionic liquid-free sample is 3.26×10^{-5} S cm^{-1}.It may be the PP1.3TFSI dissolving in the PEO, decreased the

PEO crystallization degree (crystallization is a important parameter in relation with the conductivity in PEO electrolyte system). On the other hand, the addition of ionic liquid PP13TFSI, which results in increasing the amount of TFSI$^-$ in the polymer electrolyte system, Li$^+$ ions (come from LiTFSI salt) are able to interact with more than one TFSI$^-$ anion, by the electrostatic between the ionic liquid ions and lithium salt [21], IL well improved the ion conductivity of the PEO.
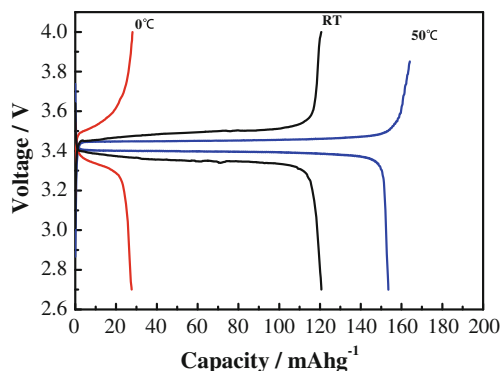
Fig. 9 Voltage–capacity plots of Li/LiFePO$_4$ cell at different temperatures

Figure 6b shows the temperature dependence of the ionic conductivity of $P(EO)_{20}LiTFSI+xPP1.3TFSI$ ($x=0$, 0.54, 0.96, 1.27). The obtained data can be fitted with the Vogel–Tamman–Fulcher (VTF) equation in the logarithmic form:

$$\sigma = A\,T^{1/2}\,\exp\left[\frac{-B}{T-T_0}\right] \qquad (2)$$

Here, A is the parameter related to the number of charge carriers, B is the activation energy for conduction, and T_0 the ideal glass transition temperature. The analysis of the experimental conductivity data in terms of the VTF relationship leads to the determination of three empirical parameters: A, B, and T_0. From the Eq. (2) and Fig.6b, we can well explain how conductivity of PEO electrolytes is influenced by ionic liquid. The B also decreases obviously with the increasing content of IL, the values of B are 0.6590 eV ($x=0$), 0.6056 eV ($x=0.54$), 0.5531 eV ($x=0.96$), and 0.4652 eV ($x=1.27$) respectively.

Transference numbers is determined by the method of Bruce et al. [17], Fig. 7a indicates that constant potential, 10 mV (ΔV), was applied across the $Li/P(EO)_{20}LiTFSI+$ $1.27PP1.3TFSI/Li$ cell until the current (I_{ss}) reached a steady state. The interfacial resistance (initial state R_0 and steady state R_{ss}) was measured by AC impedance, Fig.7b shows the impedance of the cell before and after polarization, there is no great difference between the R_0 and the R_{ss}, and this shows the stability of the lithium electrode in electrolytes based mixed ILs. The value of I_0, I_{ss}, R_0, and R_{ss} insert in Eq. (3), the lithium transference number is calculated to be 0.339, which is a acceptable value for application in lithium batteries [20].

$$t_{Li+} = I_{SS}(\Delta V - I_0 R_0)/I_0(\Delta V - I_{SS} R_{SS}) \qquad (3)$$

The voltage–capacity plots of the $LiFePO_4/Li$ cell using IL polymer electrolytes at 0.1 C charge–discharge rate are shown in Fig. 8a. As can be seen, the first charge capacity and the discharge capacity are 113 and 117 mAh g^{-1}, respectively. From 2nd cycle, the reversible capacity increases gradually. Figure 8b shows the cycle performance at the current of 0.1 C, the capacity is constant with the value of 120 mAh g^{-1} (approaching 70% of the theory capacity) even after 20 cycles and the coulomb efficiency is also higher than 99%. The fact that $LiFePO_4$ is not cycled beyond the electrochemical window of PEO-IL polymer electrolytes also works to maintain the stable cycling.

Figure 9 shows the voltage–capacity plots of $Li/P(EO)_{20}$ $LiTFSI+1.27PP1.3LiTFSI/LiFePO_4$ cell at different temperatures. As can be seen, the charge capacity and discharge capacity are greatly increasing with the temperature (charge capacity is ~164 mAh g^{-1} at 55 °C, 93% specific capacity of $LiFePO_4$). It can be said that the properties of the cell with $P(EO)_{20}LiTFSI+1.27PP1.3LiTFSI$ could be close to the half cell using the conventional organic electrolytes. A poor performance of the cell was observed at 0 °C (the discharging capacity of the $LiFePO_4$ is at the level of only 20–30 mAh g^{-1}); this is an attribute to high viscosity of IL at low temperature and the poor low temperature performance of $LiFePO_4$ cathode.

Conclusion

Solvent-free, polymer electrolytes, incorporating PP1.3TFSI were prepared and characterized. The PEO-LiTFSI-PP1.3TFSI ternary systems show good properties with a high stability even after prolonged storage and high temperature. The addition of RTILs to PEO-LiTFSI electrolytes resulted in a large increase of the ionic conductivity, thermal stability, and safety. Preliminary battery tests have shown that $Li/LiFePO_4$ solid-state cells are capable of delivering reasonable capacity (120 mAh g^{-1} at room temperatures, 164 mAh g^{-1} at 55 °C); $Li/LiFePO_4$ cell have shown the promising cycle life and higher coulomb efficiency with this ionic liquid-polymer electrolyte at room temperature.

References

1. Ding MS, Xu K, Zhang SS, Jow TR (2000) J Electrochem Soc 147:1688
2. Beaton SP, Bishop GA, Zhang Y, Ashbaugh LL, Lawson DR, Stedman DH (1995) Science 268:991
3. Kim GT, Appetecchi GB, Alessandrini F (2007) J Power Sources 171:861
4. Nishimoto A, Agehara K, Furuya N, Watanabe T, Watanabe M (1999) Macromolecules 32:1541
5. Croce F, Serraino-Fiory F, Persi L, Scrosati B (2000) Electrochem Solid-State Lett 4(8):A121
6. Saito Y, Stephan-Manuel A, Kataoka H (2003) Solid State Ionics 16:149
7. Stephan AM, Kumar SG, Renganathan NG, Kulandainathan MA (2005) J Eur Polym 41:15
8. Sakaebe H, Matsumoto H (2003) Electrochem Commun 5:594
9. Chagnes A, Carre MB (2005) J Power Sources 145:82
10. Galinski M, Lewandowski A, Stepniak I (2006) Electrochim Acta 51:5567
11. Tsunashima K, Sugiya M (2007) Electrochem Commun 9:2353
12. Seki S, Ohno Y, Kobayashi Y, Miyashiro H, Usami A, Mita Y, Tokuda H, Watanabe M, Hayamizu K, Tsuzuki S, Hattori M, Terada N (2007) J Electrochem Soc 154(3):A173
13. Kim S, Jung Y, Park S (2007) Electrochim Acta 52:2116

14. Matsumoto H, Sakaebe H, Tatsumi K (2005) J Power Sources 146:45
15. Shin JH, Henderson W, Passerini S (2005) Electrochem Solid-State Lett 8:A125
16. Kim KS, Park SY, Choi S, Lee H (2006) J Power Sources 155 (2):385
17. Evans J, Vincent CA, Bruce PG (1987) Polymer 28(13):2324
18. Fernicola A, Croce F, Scrosati B (2007) J Power Sources 174:342
19. Ramesh S, Yuen TF, Shen CJ (2008) Electrochim Acta 69:670
20. Cheng H, Zhu CB, Huang B (2007) Electrochim Acta 52:5789
21. Castriota M, Caruso T, Agostino RG, Cazzaneli E, Henderson WA, Passerini S (2005) J Phys Chem 109(1):92